Article

The Investigation of Protein Diffusion via H-Cell Microfluidics

Miao Yu,[1,*] Tiago Castanheira Silva,[1] Andries van Opstal,[1] Stefan Romeijn,[2] Hayley A. Every,[4] Wim Jiskoot,[2] Geert-Jan Witkamp,[3] and Marcel Ottens[1]

[1]Department of Biotechnology, Delft University of Technology, Delft, the Netherlands; [2]Division of BioTherapeutics, Leiden Academic Centre for Drug Research, Leiden University, Leiden, the Netherlands; [3]King Abdullah University of Science and Technology, Water Desalination and Reuse Center, Division of Biological and Environmental Science and Engineering, Thuwal, Saudi Arabia; and [4]FeyeCon Development & Implementation, Weesp, the Netherlands

ABSTRACT   In this study, we developed a microfluidics method, using a so-called H-cell microfluidics device, for the determination of protein diffusion coefficients at different concentrations, pHs, ionic strengths, and solvent viscosities. Protein transfer takes place in the H-cell channels between two laminarly flowing streams with each containing a different initial protein concentration. The protein diffusion coefficients are calculated based on the measured protein mass transfer, the channel dimensions, and the contact time between the two streams. The diffusion rates of lysozyme, cytochrome *c*, myoglobin, ovalbumin, bovine serum albumin, and etanercept were investigated. The accuracy of the presented methodology was demonstrated by comparing the measured diffusion coefficients with literature values measured under similar solvent conditions using other techniques. At low pH and ionic strength, the measured lysozyme diffusion coefficient increased with the protein concentration gradient, suggesting stronger and more frequent intermolecular interactions. At comparable concentration gradients, the measured lysozyme diffusion coefficient decreased drastically as a function of increasing ionic strength (from zero onwards) and increasing medium viscosity. Additionally, a particle tracing numerical simulation was performed to achieve a better understanding of the macromolecular displacement in the H-cell microchannels. It was found that particle transfer between the two channels tends to speed up at low ionic strength and high concentration gradient. This confirms the corresponding experimental observation of protein diffusion measured via the H-cell microfluidics.

INTRODUCTION

The diffusion of proteins is often critical in the design of mass transfer equipment, such as protein extraction and fractionation (chromatography) systems, which are widely used in (bio)chemical and biopharmaceutical industries (1). Moreover, the protein diffusion coefficient is used to estimate the molecular weight and the hydration state of proteins, the aggregation state, and the protein behavior in specific systems in which diffusion is the rate-limiting factor (for example, in some controlled drug delivery systems in which the release rate of therapeutic protein depends on its diffusion coefficient) (1–4).

In the absence of external forces, such as an electric field, at least three forces dominate the dynamics of proteins in a low-molecular-weight solvent like water (5,6): 1) Brownian motion, 2) protein-protein (electrostatic) interactions, and 3) hydrodynamic interactions due to perturbation of the solvent velocity by other protein molecules. The protein-protein interactions are dependent on the protein size, shape, surface charge, etc. This makes it complicated to generalize the diffusion behavior of proteins under various conditions regarding the impact of the forces above on the protein molecular diffusivity.

A summary of various methods for the measurement of solute diffusion coefficient has been listed elsewhere (7,8). Among these techniques, dynamic light scattering (DLS), NMR, Taylor dispersion analysis (TDA), Gouy interferometry (GI), Rayleigh interferometry (RI), and fluorescence correlation spectroscopy have all been used to determine protein diffusion coefficients (9–13). These techniques are compared in Table 1. The drawbacks of some of these techniques, such as the high equipment costs (e.g., NMR) and the need for high-quality equipment parts (e.g., the lens for RI), limit their routine use. Besides, there are some limitations on the detection of some of the listed techniques. As to light scattering methods, there are limiting factors, such

TABLE 1 Summary of the Characteristics of H-Cell Microfluidics and Other Techniques for the Determination of Protein Diffusion Coefficient

Characteristics of the Technique	DLS (7,9,14,39,70)	NMR (7,8,17)	TDA (8,13)	GI (7,8,71)	RI (7,71)	Fluorescence Correlation Spectroscopy (72–75)	H-cell
Accuracy	±[a]	+[b]	±	+	+	±	±
Measurement time consumption [c]	+	±	±	−[d]	−	±	±
Flexibility	−	−	±	NA[e]	NA	−	+
Requirement on sample properties[f]	−	NA	±	−	−	−	+
Sample consumption	±	+	+	−	−	+	+
Resolution	+	+	±	NA	NA	+	±
Data analysis	±	±	+	−	−	NA	+
Set-up cost	±	−	+	±	−	−	+
Equipment installation	±	−	+	−	−	−	+

[a]The medium level is labeled as " ± ".

[b]The "+" sign represents the advantageousness of the technique for corresponding characteristics.

[c]The duration of H-cell measurement depends on the dimension of the microfluidic channel. In this study, it took ∼1–2 h per single run for the measurement of LYS diffusion coefficients, whereas methods like DLS or NMR take about half the time. The length of each measurement can be reduced by using an H-cell of shorter span-wise dimension, in which shorter contacting time between the two laminar streams is needed. So, the microfluidics method has the potential of shortening the measurement time in the future.

[d]The "−" sign represents the disadvantageousness of the technique for corresponding characteristics.

[e]NA, not available.

[f]Such as refractive index, turbidity level, molecular size, etc.

as the following: 1) a relatively high solute concentration or large solute molecular size is required for a detectable intensity of scattering light; 2) if solute and solvent have the same refractive index, there is no contrast and, thus, no scattering light; and 3) if the turbidity of solutions is too high (e.g., emulsions), multiple scattering of light leads to measurement inconsistencies or errors (7,14). As to the TDA, the diffusion coefficient is derived from the band broadening measured by the analytical detector (e.g., ultraviolet (UV) absorbance); thus, there is a high requirement on the sensitive detection modality. Additionally, there is a need for a large sample injection volume and extended analysis time to fulfill the conditions of validity (13,15). Fluorescence methods require the dyeing of protein, which may change its properties and, thereby, protein-protein interactions (16). For NMR, local magnetic field gradients and imaging gradients as well as the length of the diffusion period have been reported to affect the measured diffusion coefficients (17). To relieve some of the drawbacks of these techniques, an orthogonal technique using a microfluidic H-cell is put forward in this study.

Prior research has shown that the application of the microfluidic method is promising for the study of solute diffusion behavior. The microscale dimensions enable a rapid detectable transport of solute molecules in the fluid. The microfluidics concept has been applied for the diffusion coefficient determination of not only common electrolytes, such as NaCl, but also macromolecules, such as proteins (18–20), in which laminar flow tubes or channels were used. The detection methods used in these studies are based on the observation of the spreading of solute bands during transport via the microfluidic devices. This type of diffusion profile in the microfluidic equipment has also been studied to characterize the sizes, interactions and aggregation state of macromolecules (e.g., proteins) (21,22) and as an indicator of the medium viscosity (23). When there are two streams introduced to a microchannel at low flow rates (laminar flow at a low Reynold number), a fluid interface is formed between the two streams, and solute transfer takes place across the interface (20,24–27). In this study, the idea of microlaminar flow is coupled with the quantitative determination of the mass transfer based on the concentration change over the length of the H-cell channel rather than the detection of molecular optical properties, such as with DLS and GI. Therefore, there is less limitation on the selection of the sample materials. Resembling the experimental schemes for solute (e.g., protein) concentration measurement in relevant microfluidics studies (28), a flexibility of mass detection methods, both online and offline, can be applied during H-cell measurement (e.g., UV-visible (UV-Vis) for protein detection in this study and conductivity detection in a previous study (29)), enabling a broader application of the microfluidic H-cell. In our lab, an H-cell (H-shape microfluidic chip) was developed and validated by Häusler et al. (29) via optimal experimental design for solute diffusion coefficient measurement. This H-cell was successfully used for the measurement of the diffusion coefficient of common electrolytes as well as polyphenols (29,30).

The goal of this study is to determine the diffusion coefficient of proteins via measuring the mass transfer between the two aqueous streams by a custom-made microfabricated H-cell and to evaluate the effectiveness of the microfluidic method for the general investigations of biomacromolecular diffusion behavior. This article starts with presenting the measured diffusion coefficients of lysozyme in different solutions (water and buffer) with different inlet concentration

TABLE 2 Experimental Operating Conditions for the H-Cell Microfluidics Study, in which the Tested Proteins, the Inlet RS and DS Concentrations, the Solvents, the NaCl Concentration for Ionic Strength Adjustment, and the Glycerol Concentration for Viscosity Adjustment Are Listed

Experiment	Protein	RS (mg/mL)	DS (mg/mL)	Solvent	NaCl (mM)	Glycerol (w/w%)
1	LYS	0	2	water	–	–
2	LYS	0	5	water	–	–
3	LYS	0	10	water	–	–
4	LYS	2	4	water	–	–
5	LYS	4	6	water	–	–
6	LYS	0	2	water	5	–
7	LYS	0	2	water	10	–
8	LYS	0	2	water	500	–
9	LYS	0	2	water	1000	–
10	LYS	0	0.5	10 & 100 mM PB[a]	–	–
11	LYS	0	1	10 & 100 mM PB	–	–
12	LYS	0	2	10 & 100 mM PB	–	–
13	LYS	0	5	10 & 100 mM PB	–	–
14	LYS	0	10	10 & 100 mM PB	–	–
15	LYS	2	4	10 mM PB	–	–
16	LYS	4	6	10 mM PB	–	–
17	LYS	0	2	10 mM PB	200	–
18	LYS	0	2	10 mM PB	500	–
19	LYS	0	2	10 mM PB	—	10
20	LYS	0	2	10 mM PB	–	20
21	LYS	0	2	10 mM PB	–	40
22	LYS	0	0.5	10 & 100 mM AC	–	–
23	LYS	0	1	10 & 100 mM AC	–	–
24	LYS	0	2	10 & 100 mM AC	–	–
25	LYS	0	5	10 & 100 mM AC	—	–
26	LYS	0	10	10 & 100 mM AC	–	–
27	LYS	2	4	10 mM AC	–	–
28	LYS	4	6	10 mM AC	–	—
29	CC	0	2	10 mM PB	–	–
30	MYO	0	2	10 mM PB	–	–
31	OVA	0	2	10 mM PB	–	–
32	BSA	0	2	10 mM PB	–	–
33	etanercept	0	2	placebo buffer	–	–

[a]The two buffers were used for experiments, respectively.

profiles for the H-cell and as a function of the medium ionic strength and viscosity. The influence of different operating conditions on the protein diffusivity is shown, and the accuracy of the method is verified via comparison of the results with published values obtained under similar conditions. Next, the applicability of the microfluidics method for a broader range of proteins is validated by measuring the diffusion coefficients of proteins with the molecular weight ranging from ~12 to 150 kDa (cytochrome c, myoglobin, ovalbumin, bovine serum albumin, and etanercept) and comparing the measured values with relevant literature values. Factors that may affect the diffusivity measurement are discussed, and exploratory numerical simulations are included.

MATERIALS AND METHODS

Materials and preparation of solutions

The proteins used in this study were as follows: lysozyme (LYS) from chicken egg white (14.3 kDa, pI ≈ 11; Sigma-Aldrich, Zwijndrecht, the Netherlands), cytochrome c (CC) from bovine heart (12.3 kDa, pI ≈ 10–11; Sigma-Aldrich), myoglobin (MYO) from horse heart (17 kDa, pI ≈ 6.8–7; Sigma-Aldrich), ovalbumin (OVA) from chicken egg white (43 kDa, pI ≈ 4.5–4.9; Sigma-Aldrich), bovine serum albumin (BSA) (66.5 kDa, pI ≈ 5–6; Sigma-Aldrich), and Enbrel (etanercept) (150 kDa, pI ≈ 8; Pfizer, Capelle aan den Ijssel, the Netherlands). Enbrel was supplied at 50 mg/mL (formulation composition is shown later), and the other proteins were supplied as dry powders.

All protein solutions (concentrations shown in Table 2) were prepared using ultrapure water (purified using a Milli-Q ultrapure water system; Millipore, Molsheim, France) as the solvent. To adjust the pH, phosphate buffer (PB) (Na_2HPO_4 and NaH_2PO_4; Sigma-Aldrich) and acetate buffer (AC) (acetic acid (Sigma-Aldrich) and sodium acetate (Merck, Darmstadt, Germany)) were used. For etanercept, a placebo buffer was used that contained 10 mg/mL sucrose (Fluka; Sigma-Aldrich, Steinheim, Germany), 5.8 mg/mL NaCl (J.T. Baker, Deventer, the Netherlands), 5.3 mg/mL arginine hydrochloride (Merck), and 3.9 mg/mL $Na_2HPO_4 \cdot H_2O$ (Sigma; Sigma-Aldrich) (pH 6.3). Furthermore, NaCl (J.T. Baker) and glycerol (Merck) were used to change the ionic strength and viscosity of the prepared protein solutions, respectively.

All the prepared solutions were filtered through 0.22-μm cellulose filters (Whatman; GE Healthcare, Little Chalfont, UK) before the experiments.
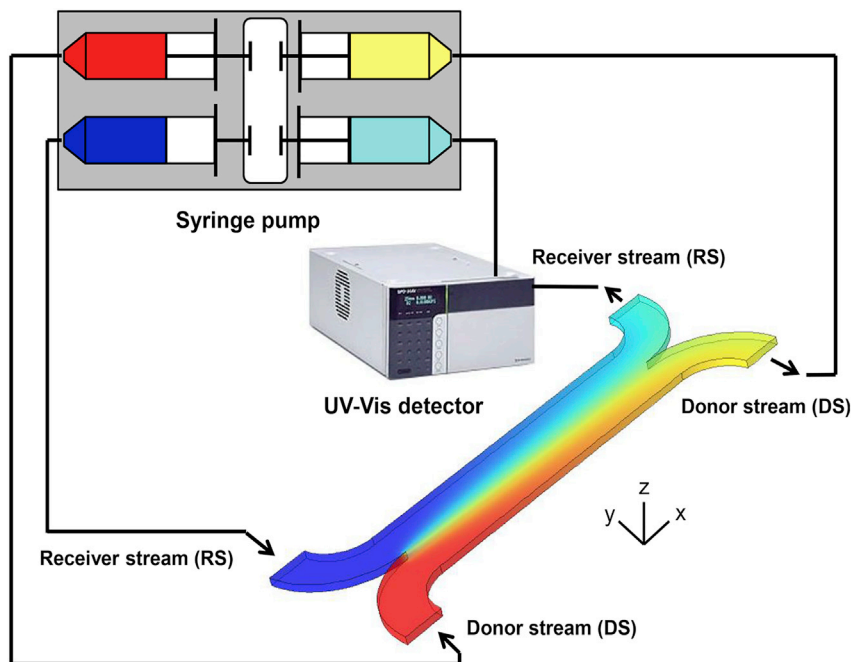
FIGURE 1 Scheme of the H-cell experimental set-up for protein diffusion coefficient measurement. The blue and cyan colors represent the inlet and outlet receiver stream (RS), respectively, and the red and yellow colors represent the inlet and outlet donor stream (DS), respectively. To see this figure in color, go online.

Experimental set-up and process description

The experimental set-up is illustrated in Fig. 1. An H-cell (Micronit, Enschede, the Netherlands) made of Borofloat glass with the dimensions 625 mm × 753 μm × 69 μm (L × W × H) was used. The dimensions were measured by using a calibrated ocular micrometer scale implemented in an Olympus microscope (Olympus, Zoeterwoude, the Netherlands).

During the experiments, a syringe pump (Model 270D; KD Scientific, Holliston, MA) introduced two streams with a protein concentration difference into the H-cell. The stream with a higher protein concentration is called as the donor stream (DS), whereas the other stream is named as the receiver stream (RS). The syringe pump injected and withdrew the streams simultaneously to maintain an equal flow ratio of the two streams during their transport in the H-cell. By implementing both the injecting syringes and sucking syringes, potential pressure-drop differences along the outlet tubes were avoided, and an equal volumetric split ratio of the DS and RS was achieved at the outlet of the channel (29). Under this condition, the solute concentration change between the DS and RS is purely a result of the solute diffusion. The input flow rate by the syringe pump was set to achieve a laminar flow profile (Reynold number less than 10). Under this condition, there was a clear interface between the two streams in the middle of the channel (a test of this interface was performed by transporting water (as RS) and an aqueous solution containing dye material (as DS) into the H-cell). The protein diffusion behavior was examined with different inlet RS and DS concentrations in various liquid media. The operating conditions are summarized in Table 2, and there were triplicate measurements for each condition.

For convenience, in this article, the inlet stream concentrations will be described as the "inlet RS concentration versus inlet DS concentration." For example, 0 vs. 2 mg/mL represents inlet concentrations of 0 mg/mL in RS and 2 mg/mL in DS.

An inline UV-Vis detector (SPD-20AV; Shimadzu) with a microflow cell (0.2 μL) was located between the H-cell and the withdrawing syringe of the RS to record the UV-Vis absorbance of the proteins. The UV-Vis detector has a sensitivity limit at the noise level of 0.5×10^{-5} AU. The microflow cell in the UV-Vis detector enables the inline detection of the proteins in the outlet stream at a low flowrate. A calibration curve was determined to correlate the UV-Vis absorbance with the protein concentration.

Protein concentration

Before the H-cell microfluidics experiments, the concentration of the prepared protein solutions was determined by a UV-Vis spectrophotometer (UV-1800; Shimadzu, Tokyo, Japan) using the wavelengths and extinction coefficients shown in Table 3.

Protein mass balance between the DS and RS

During the check of the mass balance between the DS and RS, two UV-Vis detectors were placed between the DS and RS outlets and the corresponding pulling syringes (not as shown in Fig. 1 in which only one UV-Vis detector is placed). Inline detection of the protein concentration in the two streams was performed. The outlet protein concentrations during experiments were obtained based on the calibration curves, which were determined for both detectors. As the syringe pump pushed and pulled the fluid at consistent flowrate simultaneously, the protein mass recovery was calculated according to Eq. 1.

$$Recovery\ (\%) = \frac{C_{outlet,DS} + C_{outlet,RS}}{C_{inlet,DS} + C_{inlet,RS}} \cdot 100\%, \qquad (1)$$

where C stands for the protein concentration, and the recovery is described as the percentage of the sum of outlet concentration of DS ($C_{outlet,DS}$) and

TABLE 3 Wavelengths and Extinction Coefficients Used for the Determination of Protein Concentration Measured by UV-Vis Spectrophotometer

Protein	Wavelength (nm)	Extinction Coefficient (mL cm^{-1} mg^{-1})	Reference
LYS	280	2.64	(76)
CC	550	0.68	(77)
MYO	408	11.06	(78)
OVA	280	0.73	(79)
BSA	280	0.66	(80)
etanercept	280	1.49	(81)

RS ($C_{outlet,RS}$) to the sum of the inlet concentration of both streams ($C_{inlet,DS}$ and $C_{inlet,RS}$).

High-performance size-exclusion chromatography

High-performance size-exclusion chromatography (HP-SEC) was performed to analyze the aggregation state of the protein materials as supplied from the manufacturer. The protein materials were dissolved in PB (10 mM (pH 7.2)) (except for etanercept, which was diluted in placebo buffer (pH 6.3)) and filtered through a 0.2-μm filter before measurement.

The protein samples of LYS, CC, MYO, OVA, and BSA (50 μL; ~1 mg/mL) were analyzed with a Discovery BIO Gel Filtration column (Sigma-Aldrich, St. Louis, MO). A 515 high-performance liquid chromatography pump and 717 Plus autosampler (Waters, Milford, MA) were operated at a flow rate of 0.5 mL/min. The mobile phase consisted of 100 mM sodium PB, 200 mM sodium chloride, and 0.05% (w/v) sodium azide at a pH of 7.2 and was filtered through a 0.2-μm filter before use. Chromatograms were recorded with an SPD-6AV UV detector (Shimadzu) at a wavelength of 280 nm.

For etanercept analysis (50 μL; ~2 mg/mL), a Yarra SEC-2000 size-exclusion column (Phenomenex, Utrecht, the Netherlands) was used with the running buffer composed of 50 mM phosphate, 150 mM arginine, and 0.025% NaN$_3$ at pH 6.5. UV detection was performed at 280 nm.

Viscosity measurement

The kinematic viscosity of the protein solutions with or without glycerol was determined at room temperature using an Ostwald viscometer (inside tube diameter: 0.26 mm; ROWEEL Electronic, Zhenzhou, China). Water was used as the reference.

Calculation of diffusion coefficient

Comsol Multiphysics (version 4.4; Comsol, Stockholm, Sweden), via a MATLAB (version 2017a; The MathWorks, Natick, MA) Livelink, was used to calculate the protein diffusion coefficient based on the outlet RS concentration under steady state. This method of calculation was developed and validated in previous research (29). The Comsol built-in module of Transport of Diluted Species was used to calculate the mass transfer between the RS and DS. In the case of rectangular cross-sectional dimension, a simplified solution of the Navier-Stokes equations was used (31).

The z-averaged velocity distribution along the y axis was calculated according to Eq. 2:

$$\overline{v}(y) = v\left(\frac{m+1}{m}\right)\left[1 - \left(\frac{y}{a}\right)^{m}\right], \tag{2}$$

where

$$m = 1.7 + 0.5\left(\frac{b}{a}\right)^{-1.4}, \tag{3}$$

where a and b stand for the channel halfwidth and half-height, respectively, and v stands for the stream velocity (dividing flowrate by the cross-sectional area of the channel).

In the simulation of transport of diluted species, Fick's second law was used to correlate the diffusivity with the concentration of solute from the DS to RS:

$$\overline{v}(y)\frac{\partial C}{\partial x} = D\left(\frac{\partial^2 C}{\partial y^2}\right), \tag{4}$$

where D represents the diffusion coefficient of the solute.

The outlet RS concentration, inlet RS and DS concentrations, flow rate, and channel dimensions are the input parameters for the calculation. MATLAB's fminbnd function (The MathWorks) was used to determine the minimal value of the least-square fitting of the calculated RS outlet concentration (via modeling) and the experimentally measured RS outlet concentration, in which the corresponding value of diffusion coefficient was the one measured by the microfluidic H-cell.

The dimensionless Fourier number (Fo), representing the contact time of the RS and DS during transport via the H-cell, was calculated as

$$Fo = \frac{Dt}{a^2}, \tag{5}$$

where D is the diffusion coefficient, t is the average residence time in the channel, and a is the channel halfwidth. The minimization of the measurement uncertainty (i.e., the variance of the experimental results) is achieved by operating the experiment at an optimal Fourier number range, in which the H-cell measurement sensitivity and accuracy increase drastically (29). Empirically, the range of the optimal Fourier number was determined according to Eq. 6:

$$Fo_{opt} = 0.299\left(\frac{b}{a}\right)^{-0.0983} \quad \text{for} \quad 0.05 < \frac{b}{a} < 0.1. \tag{6}$$

Based on the analysis of the Fisher information matrix (a common factor of ordinary differential equation analysis; reciprocal of the variance of measured diffusion coefficients) (29,32), the experimental check on the correlation of the Fourier number with the variance of measured protein diffusion coefficients (see Fig. S1), and the empirical correlation (Eq. 6), the Fourier number range of 0.3–0.4 was used (in which a low level of variance occurs), and the determined diffusion coefficients corresponding to this Fourier number range were reported.

Stokes-Einstein diffusion model

The Stokes-Einstein diffusion model (see Eq. 7) classically correlates the diffusion coefficient of monodisperse spheres at infinite dilution with the viscosity of the medium and the size of the molecule. The solute molecule is considered as a Brownian particle dissolved in a continuous medium. In the model, the microscopic structure of both solute and solvent is neglected, and the only source of dissipative effects is the shear viscosity of the solvent.

$$D = \frac{k_B T}{6\pi\eta R_h}, \tag{7}$$

where k_B represents the Boltzmann constant, T represents the absolute temperature, η represents the viscosity of the medium, and R_h represents the hydrodynamic radius.

For nonideal solutions like protein solutions, intermolecular interactions have an impact on the diffusion coefficient, whereby the diffusion coefficient is corrected for the concentration factor via a linear correlation (see Eq. 8):

$$D = D_0(1 + k_D C), \tag{8}$$

where D_0 is the protein diffusion coefficient at infinite dilution, and k_D is the diffusion interaction parameter summarizing protein-protein intermolecular interactions (33,34). The term k_D is used to represent the level of both direct (e.g., electrostatic, dipole-dipole, van der Waals, and hydrophobic interactions) and solvent-mediated hydrodynamic interactions among the protein molecules that alter the purely thermally driven protein motion. The value of k_D depends on factors such as the temperature and NaCl concentration in the medium.

Numerical simulation of particle diffusion

In this study, the H-cell microfluidics results indicate different diffusion behaviors of protein molecules in different buffers and protein concentrations. It is assumed that the diffusivity of protein molecules in the H-cell is affected by the protein charge, intermolecular interaction cutoff distance (Debye length), protein concentration, and concentration gradients between RS and DS. To give support to this assumption, an exploratory and illustrative numerical simulation of particle displacement (which represents the diffusion of globular protein molecules) between two contacting domains was performed.

This simulation was conducted by the particle tracing module of Comsol Multiphysics (version 5.2; Comsol). The geometrical configurations and boundary conditions of the simulation are shown in Fig. S2. The simulation geometry was divided into two domains, donor fluid domain (DD) and receiver fluid domain (RD), in which DD has a higher initial concentration than RD. In the simulation, spherical particles were used to represent protein molecules. Because of the limit on computation power, the particle displacement was simulated within a downscaled geometry rather than the full scale of the H-cell.

In the simulation, the particle displacement was dominated by three forces: Brownian force, drag force, and particle-particle interaction force (electrostatic repulsive force in this case) (35).

The amplitudes of Brownian force at every time step were modeled as a Gaussian white noise process (36) given by Eq. 9:

$$F_b = \zeta \sqrt{\frac{12\pi k_B \eta T r_p}{\Delta t}}. \qquad (9)$$

The drag force was given by Eq. 10:

$$F_d = \left(\frac{1}{\tau_p}\right) m_p (v - v_p). \qquad (10)$$

Coulombic force dominates particle-particle interaction and is repulsive with particles of the same sign of charge. The Coulombic force was calculated with Eq. 11 as the interaction of point charges, in which the charge number was used as the charge exposed to the surface of the protein molecule:

$$F_i = -\frac{1}{4\pi\varepsilon_0\varepsilon_r} e^2 \sum_{j=1}^{N} Z_i Z_j \frac{(r_i - r_j)}{|r_i - r_j|^3}, \qquad (11)$$

where m_p is the particle mass, r_p is the particle radius, τ_p is the particle velocity response time, v_p is the velocity of the particle, v is the fluid velocity, Δt is the magnitude of the time step taken by the solver, ζ is a vector of independent normally distributed random numbers with zero mean and unit SD, e is the elementary charge, ε_0 is the permittivity of free space, ε_r is the relative permittivity of water, Z is the particle charge number, r_i is the position vector of the i-th particle, and r_j is the position vector of the j-th particle.

The diffusion of LYS in 10 and 100 mM AC, and 10 and 100 mM PB was simulated. The simulation conditions are listed in Table 4.

RESULTS

The relative size and aggregation state of proteins

Fig. 2 shows the HP-SEC chromatograms of the proteins used in this study. According to the retention time, the size of proteins follows the following order: LYS < CC < MYO < OVA < BSA < etanercept. This order is in line with the molecular weight of the proteins, except for the LYS and CC, in which CC theoretically should have a slightly smaller size (~2 kDa difference).

Narrow sharp peaks in the chromatogram of LYS and CC indicate monodisperse protein molecules. For the other proteins, some aggregations occur, based on the multipeaks shown in Fig. 2. However, the proteins are primarily in the monomeric form, based on the areas of the peak (LYS and CC: ~100%; MYO: ~88%; OVA: ~83%; BSA: ~70%; etanercept: ~95%). The determined diffusion coefficients in this study reflect majorly the diffusion behavior of monomeric protein molecules.

TABLE 4   The Conditions Used for Comsol Particle Tracing Simulation

Simulation	Simulated Solvent	RD Concentration (mg/mL)[a]	DD Concentration (mg/mL)	Medium Viscosity (mPa·s)[b]	Particle Charge Number[c]	Cutoff Distance (nm) (Coulombic Interaction)[d]
1	AC (10 mM; pH 4.2)	0	2	1.00	15.2	6.8
2	AC (10 mM; pH 4.2)	0	10	1.00	15.2	6.8
3	AC (10 mM; pH 4.2)	2	4	1.00	15.2	6.8
4	AC (10 mM; pH 4.2)	4	6	1.00	15.2	6.8
5	AC (100 mM; pH 4.2)	0	2	1.02	15.2	2.0
6	AC (100 mM; pH 4.2)	0	10	1.02	15.2	2.0
7	PB (10 mM; pH 7.2)	0	2	1.00	11.1	2.1
8	PB (10 mM; pH 7.2)	0	10	1.00	11.1	2.1
9	PB (10 mM; pH 7.2)	2	4	1.00	11.1	2.1
10	PB (10 mM; pH 7.2)	4	6	1.00	11.1	2.1
11	PB (100 mM; pH 7.2)	0	2	1.06	11.1	0.6
12	PB (100 mM; pH 7.2)	0	10	1.06	11.1	0.6

[a]The experimental solute concentration is converted to the number of particles per volume for the simulation via the correlation $C_n = C_e \times N_A/M_w$, in which C_n represents the particle number concentration used for the simulation, C_e represents the experimental solute concentration, N_A represents the Avogadro number, and M_w represents the molecular weight of solute.

[b]The medium viscosity is calculated based on the table of the properties of the aqueous solutions of common electrolytes shown in (82).

[c]The particle surface charge is calculated based on the pKa of protein amino acid residues and their corresponding buried percentage obtained from the online PDB2PQR Server (PDB2PQR Version 2.0.0 (83)).

[d]The calculated ionic strength of 10 and 100 mM AC is 2 and 24 mM, respectively; for PB, the value is 21 and 221 mM, respectively (calculated via (84)). The Debye length is calculated based on these ionic strengths using the equation $\delta = \sqrt{\varepsilon_r \varepsilon_0 k_B T/2 N_A e^2 I}$, in which δ represents the Debye length, ε_r represents the relative permittivity of water, ε_0 represents the permittivity of free space, k_B represents Boltzmann constant, T represents the temperature, N_A represents the Avogadro number, e represents the elementary charge, and I represents the ionic strength.
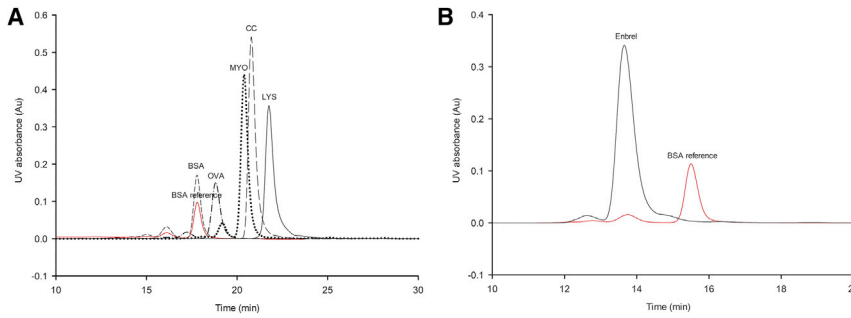
FIGURE 2 HP-SEC chromatograms of proteins used for the H-cell diffusion experiments. (*a*) Chromatogram of LYS, CC, MYO, OVA, and BSA, together with a BSA reference (*b*) Chromatogram of etanercept and the corresponding BSA reference. To see this figure in color, go online.

Protein mass balance

The recovery of proteins after flowing through the H-cell is shown in the Table S2. Under all test conditions, the protein recoveries at the outlets of the DS and RS were not significantly different from 100% according to the *t*-test ($p > 0.05$).

LYS diffusion coefficient as a function of concentration, pH, and buffer type

LYS diffusion coefficients in water, PB and AC, were measured by the H-cell microfluidics device at different inlet concentrations of the DS and RS. The results are shown in Fig. 3.

LYS diffusion in water

For LYS, a diffusion coefficient of 4.4×10^{-10} m^2/s was measured at 0 vs. 2 mg/mL, which is in line with published data (10) (37,38). More than 50% increase of the measured diffusion coefficient was observed at 0 vs. 5 and 0 vs. 10 mg/mL.

When the inlet concentration gradient between the RS and DS was kept at 2 mg/mL, almost no difference in the diffusion coefficient was observed between 0 vs. 2, 2 vs. 4, and 4 vs. 6 mg/mL. LYS was reported to have a diffusion coefficient of $\sim 5.5 \times 10^{-10}$ m^2/s in water via DLS and GI measurement at similar levels of concentrations (<10 mg/mL) (37,38). However, even with the same diffusion measurement method (GI), a diffusion coefficient of 2.2×10^{-10} m^2/s was reported in another previous study (10). The measured LYS diffusion in water was more influenced by the protein concentration gradient between the RS and DS than by the absolute protein concentrations in the H-cell channel.

LYS diffusion in AC

In 10 mM AC, LYS diffusion coefficients in the range of $1.6–2.1 \times 10^{-10}$ m^2/s were obtained at 0 vs. 0.5 to 0 vs. 2 mg/mL. Similar diffusion coefficients have been reported in previous publications under the conditions of similar pH and ionic strength (39,40). Inlet concentration gradients of up to 2 mg/mL did not substantially affect the measured

diffusion coefficients. However, at higher concentration gradients (0 vs. 5 and 0 vs. 10 mg/mL), higher diffusion coefficients up to $\sim 3.4 \times 10^{-10}$ m^2/s were observed.

At constant inlet concentration gradient, the measured diffusion coefficients increased with increasing LYS concentration from 0 vs. 2 to 4 vs. 6 mg/mL. This trend differs from the case in water.

The measured LYS diffusion coefficients in 100 mM AC were similar to those in 10 mM AC from 0 vs. 0.5 to 0 vs. 2 mg/mL. There was no obvious trend of increasing diffusion coefficient from 0 vs. 2 to 0 vs. 5 and 0 vs. 10 mg/mL. The diffusion of LYS in AC at a low buffer concentration tended to be more influenced by the concentration gradient between RS and DS than that at high buffer concentration. Also, at a low buffer concentration, the LYS concentration in the H-cell channel proportionally affected its measured diffusion coefficient.

LYS diffusion in PB

The measured diffusion coefficients of LYS in PB were comparable with those in AC at inlet concentrations of 0 vs. 0.5, 0 vs. 1, and 0 vs. 2 mg/mL. At the inlet concentrations of 0 vs. 5 and 0 vs. 10 mg/mL, the measured values in PB were similar to those in 100 mM AC but lower than those in 10 mM AC. In 100 mM PB, the measured diffusion coefficients of LYS decreased by $\sim 25\%$ from a low concentration gradient (0 vs. 0.5 to 0 vs. 2 mg/mL) to a high concentration gradient (0 vs. 10 mg/mL). This decrease was not obvious under the other tested conditions.

When keeping the inlet concentration gradient at 2 mg/mL, an increasing diffusion coefficient with LYS concentration was observed, similar to that in AC. This trend of concentration dependency was also reported elsewhere in a low ionic strength media (with the ionic strength lower than the 10 mM PB) (41).

The diffusion of LYS in PB at low and high buffer concentrations was not much affected by the concentration gradient between RS and DS. However, the measured diffusion coefficients rose with the LYS concentration in the H-cell channel.

In light of the results above, the measured diffusion coefficients of LYS are affected by the concentration gradient
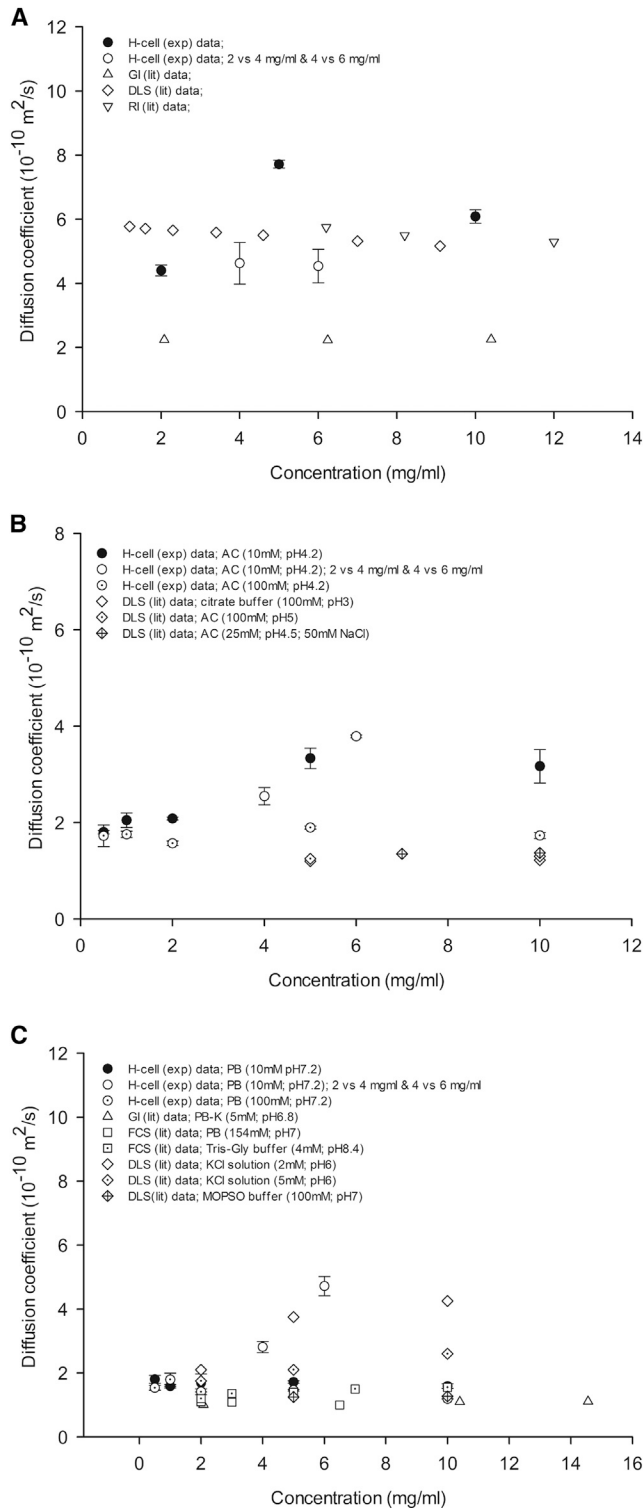
FIGURE 3 H-cell microfluidics experimental results of LYS diffusion coefficients in water (*a*), acetate buffer (AC) (*b*), and phosphate buffer (PB) (*c*) as a function of inlet concentrations. The error bars represent the standard deviation of the measurements. The *x* axis corresponds to the inlet LYS concentration in the DS. If not explicitly stated, the inlet LYS concentration in the RS is 0 mg/mL. The literature-reported LYS diffusion coefficients, measured by other techniques under similar conditions, are shown for comparison. In (*a*), the data of the triangles are collected from (10), di-

between the RS and DS, the concentration of protein in the H-cell channel, and the buffer pH and concentration. It seems that at a low protein concentration and concentration gradient (e.g., 0 vs. 0.5, 0 vs. 1, and 0 vs. 2 mg/mL), the H-cell performs well in the measurement of protein diffusion coefficients, which are comparable with literature data.

LYS diffusion coefficient as a function of ionic strength

The results in the last section indicate that there is a correlation between the measured LYS diffusion coefficient and the buffer concentration. In this section, the H-cell is used to examine the LYS diffusion coefficients at different NaCl concentrations to elucidate whether specific buffer effects or general ionic strength effects are responsible for the above observation.

The ionic strength of the medium was changed by adjusting the salt (NaCl) concentration. The measured LYS diffusion coefficients in the corresponding media are reported (see Fig. 4, *a* and *b*). As indicated by both the H-cell results and literature data, the value of the LYS diffusion coefficient sharply decreases with increasing NaCl concentration from 0 to ~10 mM, followed by leveling off at higher NaCl concentrations. In the absence of NaCl, the H-cell gave a diffusion coefficient of 4.4×10^{-10} m^2/s for LYS in water. When the NaCl concentration increased to 10 mM in water, the H-cell measured LYS diffusion coefficient dropped to lower than 2×10^{-10} m^2/s, which was similar to the diffusion coefficient measured in PB (10mM; pH 7.2). At higher NaCl concentrations (up to 1 M in water and 500 mM in PB), the LYS diffusion coefficient leveled off at ~1.6×10^{-10} m^2/s.

LYS diffusion coefficient as a function of medium viscosity

The diffusion coefficient is inversely proportional to the medium viscosity as indicated by the Stokes-Einstein model. Measuring the LYS diffusion coefficients in different viscous media can be used as a further validation of the H-cell. The diffusion coefficients of LYS are plotted against the viscosity of the solution containing glycerol (see Fig. 5). As expected, the diffusion coefficients decrease with increasing medium viscosity. A comparison of the measured diffusion coefficients to the values calculated by classical Stokes-Einstein model is presented. The molecule of LYS can be considered to be roughly spherical because of its compact nature and rapid rotational tumbling in solution (42). The reported hydrodynamic radius (R_h) of LYS differs

amonds from (37), and inverted triangle from (38). In (*b*), the data of the diamonds and dotted diamonds are collected from (39), and the crossed diamonds from (43). In (*c*), the data of the triangles are collected from (10), crossed diamonds from (39), square and dotted squares from (85), and the others from (41).
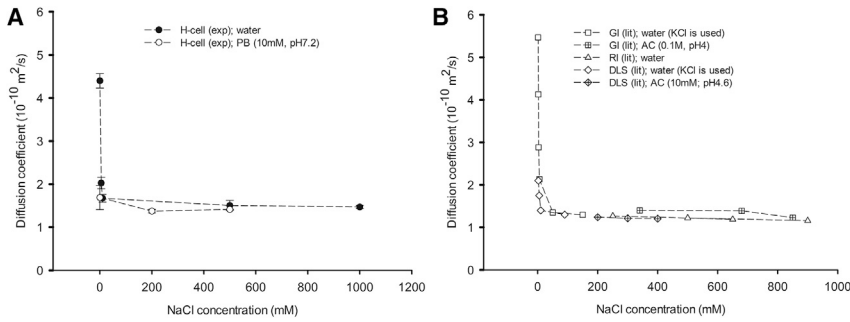
FIGURE 4 Measured diffusion coefficients of LYS via the H-cell as a function of salt concentration in the medium (*a*). The error bars represent the standard deviation of the measurements. The literature-reported LYS diffusion coefficients measured by other techniques under similar conditions (*b*) are shown for comparison, in which the data of the squares are collected from (37), crossed squares from (86), triangles from (9), diamonds from (41), and crossed diamonds from (45). The solvents used in these references are depicted in the legend of the graph. The dashed lines are meant for visual guidance.

in the literature, ranging from ∼16 to 21 Å, depending on the solvent conditions such as pH, salt types and concentrations, and experimental techniques (9,33,43,44). This size range was used for the Stokes-Einstein modeling of the diffusion coefficients in this study. The modeling results are also displayed in Fig. 5. The H-cell results are in accordance with the modeling results at the R_h of 1.6 nm. The modeling results are lower than the H-cell results at a higher R_h. The correction of concentration effect based on empirical Eq. 8 slightly lifts the value of modeling diffusion coefficients, in which an approximate value of 10 was used for the diffusion interaction parameter (kD) for a buffer condition at about pH 7 and a low ionic strength (<10 mM) (43,45). According to the results corrected for concentration, the hydrodynamic radius of LYS is predicted to be between 1.6 and 1.8 nm, which is consistent with the previously reported value of the hydrodynamic size of LYS measured in PB via TDA (46). The difference of the diffusion coefficient between measurement and modeling depicted in this study was also observed in a previous publication (47). According to the analysis above, one of the

possible factors causing this deviation is the value of the hydrodynamic radius used for the calculation.

The independence of the calculated protein size on the medium viscosity is another verification of the applicability of the H-cell for the diffusion coefficient measurement. A Spearman correlation analysis was conducted (IBM SPSS 24; IBM, Armonk, NY) on the variables of the viscosity and the hydrodynamic radius (R_h) of the protein calculated via the Stokes-Einstein equation based on the H-cell measured diffusion coefficients. It was demonstrated that there was no significant statistical correlation ($p > 0.05$) between the medium viscosity and the calculated protein hydrodynamic radius based on the measured diffusion coefficients.

The diffusion coefficient of other proteins

Besides LYS, five other proteins with different molecular size and properties (e.g., pI) were measured via H-cells for their diffusion coefficients (see Fig. 6). As expected, the diffusion coefficients of proteins were inversely related to the molecular size, in which the larger the protein (as indicated by the HP-SEC results shown in Fig. 2), the slower the detected protein diffusion. For CC and MYO, deviations, at most 20%, of the H-cell results with literature value were found. For OVA, BSA, and etanercept, quite similar values were reported in previous research (less than 10% difference) to the H-cell results. The fraction of monomeric BSA was separated and collected (see chromatogram in Fig. S4) and was measured by H-cell microfluidics. The obtained diffusion coefficient (6.7×10^{-11} m^2/s) was slightly higher than that of the unfractionated BSA (5.8×10^{-11} m^2/s), which includes dimers and trimers. In light of the comparable results generated by H-cell and other available techniques, the effectiveness and validity of the H-cell for the evaluation of protein diffusion behavior are further demonstrated.
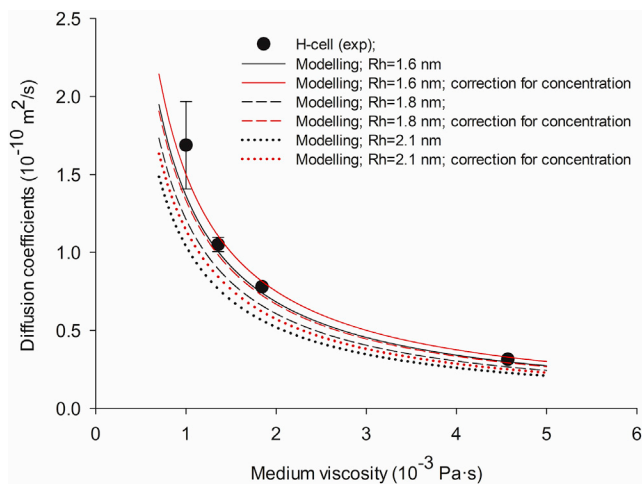

FIGURE 5 Diffusion coefficients of LYS measured by H-cell as a function of medium viscosity adjusted by glycerol. The error bars represent the standard deviation of the measurements. The diffusion coefficients calculated by the Stokes-Einstein equation are shown with the hydrodynamic radius (R_h) of 1.6 ∼ 2.1 nm. A correction of protein concentration by diffusion interaction parameter (43,45) is also included. To see this figure in color, go online.

Particle tracing simulation

Particle tracing simulation provides support for a better understanding of the protein diffusion results by counting particle transport between two contact simulation domains with an initial concentration difference. According to the
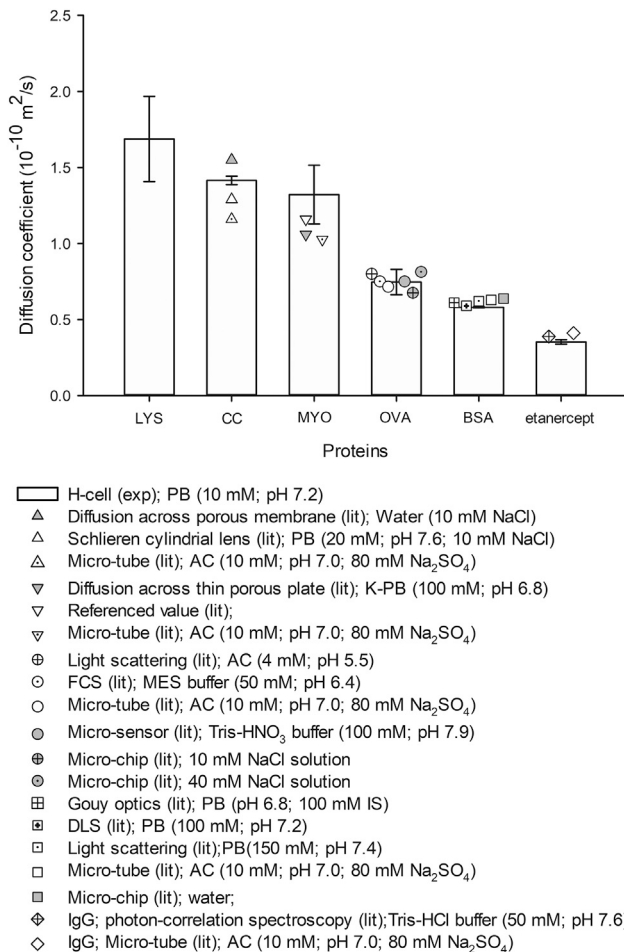
FIGURE 6 Diffusion coefficients of different proteins measured in phosphate buffer ((PB) 10 mM; pH 7.2; except for etanercept in placebo buffer) and literature-reported values under similar conditions. The error bars represent the standard deviation of the measurements. The data of the gray triangles are collected from (87), blank triangle from (88), dotted triangle from (18), gray inverted triangle from (89), blank triangle from (90), dotted triangle from (18), crossed circle from (91), dotted circle from (12), blank circle from (18), gray circle from (20), crossed gray circle and dotted gray circle from (19), crossed square from (92), x-haired square from (93), dotted square from (94), blank square from (18), gray square from (19), crossed diamond from (95), and blank diamond from (19). Because of limited information on the diffusion coefficient of etanercept, the diffusion coefficient of IgG with similar molecular size (~150 kDa) is used for comparison to the H-cell measurement results.

simulation results (see Fig. S3; Table S1), the particles diffused faster in 10 mM AC than in the other buffers. In 10 mM AC, the diffusion rate of LYS at 0 vs. 10 mg/mL was higher than that at 0 vs. 2 mg/mL. This increment as a function of concentration gradient was also observed in the case of 100 mM AC and slightly 10 mM PB but did not occur for the 100 mM PB, in which the diffusion rate decreased with the increasing concentration gradient. In the case of 10 mM AC and 10 mM PB, particles diffused faster at 4 vs. 6 mg/mL than that at 2 vs. 4 mg/mL, and both were faster than that at 0 vs. 2 mg/mL.

DISCUSSION

General

When present in solution, protein diffusion depends not only on the viscosity of the medium but also the protein-protein interactions, which are related to the strength of the interaction and the concentration of the solutes. To provide an overview of the applicability and potential of the H-cell microfluidics device on the determination of protein diffusivity, the diffusion coefficients of model protein (LYS) were measured in different media (water, PB, AC) at different pH (4.2 and 7.2), ionic strength (NaCl concentration of 0–1 M), viscosity (1–5 mPa·s), and protein concentration profiles (0 vs. 2 to 0 vs. 10 mg/mL; 2 vs. 4 mg/mL; 4 vs. 6 mg/mL). For the proof of the H-cell applicability to a broad scope of proteins with different properties (e.g., molecular weight), five other proteins were also tested via H-cell, and the measured diffusion coefficients were comparable to studies elsewhere (the characteristics of the techniques applied to determine the protein diffusion coefficients are summarized in Table 1). The key factors that influence protein diffusion and the interpretation of the H-cell results are discussed in the following sections.

Interaction among protein molecules in different media

The diffusion behavior of LYS, depicted in Fig. 3, varied in water, AC (10 and 100 mM), and PB (10 and 100 mM). The measured diffusion coefficients of LYS as a function of the solvating medium followed the order of water >10 mM AC > 100 mM AC ≥ 10 mM PB > 100 mM PB in the cases in which the inlet RS concentration is 0 mg/mL. The differences in different media were more evident at high concentration gradients than at low gradients. When in the concentration profile of 2 vs. 4 and 4 vs. 6 mg/mL, similar diffusion behaviors were found in 10 mM AC and 10 mM PB.

There is a slight change in the viscosity of different media. The 100 mM PB and 100 mM AC have ~6 and 2% higher viscosity than that of water, 10 mM PB, and 10 mM AC, which have almost similar viscosity. Thus, the slight viscosity change cannot explain all the differences of the measured diffusion coefficients, especially the ones in water and 10 mM AC (0 vs. 5 and 0 vs. 10 mg/mL), which show more than 50% higher value than the ones in the other media.

Besides viscosity, intermolecular interactions (e.g., electrostatic repulsion) among the proteins, which are influenced by both the pH and ionic strength of the medium, contribute partly to the aforementioned diffusivity difference. The impact of pH depends on the specific surface configuration (such as the fraction of exposed amino acid residues chargeable at the specific pH) of the studied protein and its resulting isoelectric point (pI; representing the pH at which the protein is electrically neutral). In water, AC

(pH 4.2), and PB (pH 7.2), LYS molecules (pI $\approx$ 11) are positively charged, and repulsive electrostatic interactions likely occur (10,48). However, when the pH is closer to the proteins' pI, the intermolecular electrostatic interaction is reduced; meanwhile, the attractive short-range interactions (interaction force decreases with distance quickly), such as van der Waals or hydrophobic forces, are relatively dominant (49). This is reasonable because the pH influences the protonation of ionizable amino acids and thus the charge distribution on the protein surface and the hydrophobic surface patches (50,51). These forces tend to hinder the dispersion and displacement of the protein molecules, opposite to the effect of repulsive interactions. As a result, relatively low diffusion coefficients tend to occur at high pH than at low pH.

The aforementioned intermolecular electrostatic repulsion can be relieved by salt screening in a medium with a relatively high ionic strength. The addition of salt is known to promote attractive hydrophobic protein interactions because of the shielding of electrostatic charges (with the same sign) (33,52).

The H-cell results of LYS diffusion with different ionic strengths (adjusted by NaCl) show slower LYS diffusion at higher NaCl concentrations. In this study, the LYS diffusion coefficient was observed to drop markedly from 4.4 $\times$ 10^{-10} to 2.0 $\times$ 10^{-10} and then to 1.7 $\times$ 10^{-10} m^2/s as the NaCl concentration increased from 0 to 5 mM and then to 10 mM (see Fig. 4), which was also observed elsewhere (37,53).

In water, the measured LYS diffusion coefficients were higher than that in AC and PB. The electrostatic free energy of the charged macromolecules increases because the charges on the macromolecules are no longer shielded from one another (37). The increased intermolecular repulsive electrostatic interactions drive the molecules strongly to displace more quickly and more frequently toward the location with fewer repulsions, which is depicted as the higher measured molecular diffusion coefficient via the H-cell.

The measured diffusion coefficients of proteins in AC were in most cases higher than that in PB. Apart from the aforementioned ion shielding effect, the type of salt may also contribute to the different diffusion behavior in different buffers. Hofmeister (54) pioneered the study and proposed the series of salts that have different abilities to salt out proteins. The mechanism of the Hofmeister series has not been entirely clarified. It was put forward that the interactions between ions and proteins, as well as ions and the water molecules that directly contact the proteins, play a role (55). According to the research, phosphate anions (HPO$_4$$^{2-}$/H$_2PO_4$$^-$/PO$_4$$^{3-}$) have a stronger tendency of salting out protein than acetate anions (56,57). This tendency may help to partly explain why the LYS molecules diffuse slightly faster in AC than in PB.

Based on the analysis above, the diffusion behavior of the protein depends on this solution condition (e.g., pH, ionic strength, salt type) and the resulting molecule properties. Electrostatic as well as additional short-range interactions play a role for the samples investigated in this study.

Concentration-dependent protein diffusion coefficients

In this study, the measured protein diffusion coefficients by H-cell depend both on the initial protein concentration gradient and the protein concentrations.

In water and AC (10 mM; pH 4.2), in which the ionic strength is low, the measured diffusion coefficients of LYS increased as the concentration gradient increased (from 0 vs. 2 to 0 vs. 5 mg/mL, as shown in Fig. 3). However, for the other buffers with a relatively high ionic strength, this elevation was not detected. The particle tracing simulation results supported the phenomena above in which the inlet concentration gradient influences the measured diffusion coefficient more in the situation of longer particle-particle interaction cutoff distance (Debye length). For example, in 10 mM AC, the cutoff distance is $\sim$6.8 nm, which is longer than the other buffers, and the particle diffusion rate is higher. When the intermolecular interaction is weakened (e.g., in 100 mM AC and 10 mM PB in which the cutoff distances are shorter ($\sim$2 nm)), the concentration gradient seems to exert less influence on the measured molecular diffusion coefficient.

The diffusion coefficients of LYS were also studied as a function of the protein concentration at consistent inlet concentration gradient (2 mg/mL). In AC and PB, the measured diffusion coefficient values increased with increasing concentration. It has previously been reported that for AC (45,58) and PB (41) at a low ionic strength, the diffusion coefficient of LYS increases with concentration, and at a higher ionic strength, this trend becomes weaker or is even independent of protein concentration. However, the level of increase reported elsewhere is less than the H-cell findings at a similar pH and ionic strength. This is probably because the high protein concentrations cause a higher frequency of collisions and, thus, the faster displacement of the molecules.

Under the investigated diffusion conditions, the effect of excluded volume (the volume that is inaccessible to other molecules in the system as a result of the presence of the first molecule; steric hindrance) seems to be less significant than the electrostatic effects. In previous research, there were statements pointing out that the increase in protein concentration promotes the impact of excluded-volume effects and additional attractive short-range interactions, therefore impeding the diffusion of the macromolecules (59,60). Usually, when the concentration of protein molecules increases to an even higher level (e.g., 20–30% v/v), the protein diffusion is retarded by the crowding of molecules (in the strict sense of excluded volume); as a result,

the stronger the electrostatic repulsions among the molecules, the more decrease of the diffusivity with the similar increase of concentration (61,62).

In water, the measured diffusion coefficients of LYS were slightly affected by the concentration (0 vs. 2, 2 vs. 4, and 4 vs. 6 mg/mL). Similar behavior was also reported previously (10,37,38) at this low concentration range. Although there is strong electrostatic repulsive interaction among the molecules and a low level of excluded-volume effect occurs in this situation, there is no similar trend of increasing diffusion coefficients as that in 10 mM PB and 10 mM AC. Scarce theoretical support for this observation is collected up to now. Regarding the presence of external salts in AC and PB, the diffusion of proteins can be accelerated by the presence of more counterions, which is a thermodynamic effect brought about by an increase in the free-energy gradient of the solutes, which is the driving force for isothermal diffusion (63). Moreover, the diffusion of proteins is likely to be enhanced or hindered by gradients of other diffusing species in the multicomponent system. The flux of the protein is related to its own concentration gradient without disturbance of the extra ions in the binary system of LYS and water. In the ternary systems of protein-salt-water, there are many counterions in the motion sphere of the protein molecule. Directly proportional to the LYS gradient, there is also an effective concentration gradient of salt. This raises the likelihood that the protein diffusion is enhanced or hindered by gradients of other diffusing species and, thus, a variation of the diffusion coefficients occurs (38,64).

The analysis above on the correlation of the concentration dependence of the protein diffusion coefficients with the intermolecular interactions provides an insight of the possible reasons explaining the H-cell observations. As the H-cell results only reflect the overall interactions among the protein molecules, the impact of each specific factor on the determined diffusion coefficient cannot be independently distinguished.

Model to calculate the diffusion coefficient

Fick's law was used to describe the diffusion of solute in the H-cell and to calculate the corresponding diffusion coefficient based on mass transport in the microscale geometry within a period. The diffusion behavior was a result of a protein concentration difference, especially for binary systems.

If we take into account the diffusion of the solvent molecules (e.g., water) besides the protein molecule transport, there is a drift flux caused by the displacement of the solvent simultaneously when protein diffuses. This drift flow is usually taken into account with gas transport rather than with a liquid system (65), and a correction factor for Fick's law diffusion is applied. However, because of the low concentration of proteins applied in the H-cell study (e.g., 10 mg/mL in water), this correction factor only causes ~1% difference to the value predicted by Fick's law.

The aforementioned drift flux is covered by the theory of Maxwell-Stefan (M-S) for the description of multicomponent diffusion behaviors (mostly applied for gas conditions). The M-S approach differs from the Fickian case because the transport is driven by a gradient in chemical potential and provides a physically based comprehensive framework to describe multicomponent mass transport. The approach relates the driving force for diffusion of one component (i.e., the chemical potential gradient at a constant temperature and pressure) to friction forces of the molecules of other components (66). Regarding the nonideal effects of mixing, the molar-based concentrations used in Fick's law are not convenient forms of thermodynamic activity variables (67). The M-S framework separates the ideal and nonideal effects of diffusion, and a thermodynamic factor is used to correlate the M-S with the Fickian case. In the case of LYS diffusion in water at 0 vs. 10 mg/mL, the M-S diffusion coefficient is calculated to be ~10% lower than by Fick's law because of the thermodynamic factor by applying the LYS activity as shown in (68). However, it was pointed out in a previous study that the thermodynamic factor involves the first derivative of the activity coefficient with respect to the composition, and errors of ~20% are expected for this derivative (66). Even taking these errors into account, the correction of the diffusion coefficient by the M-S theory is not sufficient to explain some of the observed phenomena, such as the elevation of the measured diffusion coefficients between 0 vs. 2 and 0 vs. 10 mg/mL in water and 10 mM AC.

CONCLUSIONS

A microfluidic H-cell was used for the determination of protein diffusion coefficients based on the mass transport via the interface between the two laminar cocurrent fluid streams in the channel. For LYS as a model protein, the measured diffusion behavior in the microfluidic H-cell was found to be influenced not only by the buffer type, pH, viscosity, and ionic strength but also by the operating conditions such as the inlet concentration gradients between the RS and DS. There was the presence of intermolecular (protein-protein) interactions during the protein diffusion in the channel. In good agreement with relevant research, the H-cell performed well to measure the diffusion coefficients of not only LYS but also some other common proteins with different molecular sizes and properties. These results prove the potential of this technique to be used as a general and promising approach for the determination of (macromolecular) diffusion coefficients.

SUPPORTING MATERIAL

AUTHOR CONTRIBUTIONS

M.Y., H.A.E., W.J., G.-J.W., and M.O. designed the research. M.Y., T.C.S., A.v.O., and S.R. carried out all experimental work and simulations, and analyzed the data. M.Y. wrote the article.

SUPPORTING CITATIONS

Reference (69) appears in the Supporting Material.

REFERENCES

1. Brune, D., and S. Kim. 1993. Predicting protein diffusion coefficients. *Proc. Natl. Acad. Sci. USA.* 90:3835–3839.

2. Nesmelova, I. V., V. D. Skirda, and V. D. Fedotov. 2002. Generalized concentration dependence of globular protein self-diffusion coefficients in aqueous solutions. *Biopolymers.* 63:132–140.

3. Price, W. S. 2007. Diffusion-based studies of aggregation, binding and conformation of biomolecules: theory and practice. *In* eMagRes. R. K. Harris and R. L. Wasylishen, eds. Wiley https://doi.org/10.1002/9780470034590.emrstm0115.

4. Langer, R. 1990. New methods of drug delivery. *Science.* 249:1527–1533.

5. Gallagher, W. H., and C. K. Woodward. 1989. The concentration dependence of the diffusion coefficient for bovine pancreatic trypsin inhibitor: a dynamic light scattering study of a small protein. *Biopolymers.* 28:2001–2024.

6. Pecora, R. 2013. Dynamic Light Scattering: Applications of Photon Correlation Spectroscopy. Springer Science+Business Media, Berlin, Germany.

7. Cussler, E. L. 2009. Diffusion: Mass Transfer in Fluid Systems, Third Edition. Cambridge University Press, Cambridge, UK.

8. Bedeaux, D., S. Kjelstrup, and J. Sengers. 2015. Experimental Thermodynamics Volume X: Non-Equilibrium Thermodynamics with Applications. Royal Society of Chemistry, London, UK.

9. Annunziata, O., D. Buzatu, and J. G. Albright. 2005. Protein diffusion coefficients determined by macroscopic-gradient Rayleigh interferometry and dynamic light scattering. *Langmuir.* 21:12085–12089.

10. Kim, Y.-C., and A. S. Myerson. 1994. Diffusivity of lysozyme in undersaturated, saturated and supersaturated solutions. *J. Cryst. Growth.* 143:79–85.

11. Yao, S., D. K. Weber, …, D. W. Keizer. 2014. Measuring translational diffusion coefficients of peptides and proteins by PFG-NMR using band-selective RF pulses. *Eur. Biophys. J.* 43:331–339.

12. Krouglova, T., J. Vercammen, and Y. Engelborghs. 2004. Correct diffusion coefficients of proteins in fluorescence correlation spectroscopy. Application to tubulin oligomers induced by Mg2+ and Paclitaxel. *Biophys. J.* 87:2635–2646.

13. Hawe, A., W. L. Hulse, …, R. T. Forbes. 2011. Taylor dispersion analysis compared to dynamic light scattering for the size analysis of therapeutic peptides and proteins and their aggregates. *Pharm. Res.* 28:2302–2310.

14. Øgendal, L. 2019. Light scattering: a brief introduction. University of Copenhagen. http://www.nbi.dk/~ogendal/personal/lho/LS_brief_intro.pdf .

15. Saetear, P., J. Chamieh, …, H. Cottet. 2017. Taylor dispersion analysis of polysaccharides using backscattering interferometry. *Anal. Chem.* 89:6710–6718.

16. Toseland, C. P. 2013. Fluorescent labeling and modification of proteins. *J. Chem. Biol.* 6:85–95.

17. Hrabe, J., G. Kaur, and D. N. Guilfoyle. 2007. Principles and limitations of NMR diffusion measurements. *J. Med. Phys.* 32:34–42.

18. Walters, R. R., J. F. Graham, …, D. J. Anderson. 1984. Protein diffusion coefficient measurements by laminar flow analysis: method and applications. *Anal. Biochem.* 140:190–195.

19. Culbertson, C. T., S. C. Jacobson, and J. Michael Ramsey. 2002. Diffusion coefficient measurements in microfluidic devices. *Talanta.* 56:365–373.

20. Kamholz, A. E., E. A. Schilling, and P. Yager. 2001. Optical measurement of transverse molecular diffusion in a microchannel. *Biophys. J.* 80:1967–1972.

21. Arosio, P., T. Müller, …, T. P. Knowles. 2016. Microfluidic diffusion analysis of the sizes and interactions of proteins under native solution conditions. *ACS Nano.* 10:333–341.

22. Kopp, M. R., A. Villois, …, P. Arosio. 2018. Microfluidic diffusion analysis of the size distribution and microrheological properties of antibody solutions at high concentrations. *Ind. Eng. Chem. Res.* 57:7112–7120.

23. Arosio, P., K. Hu, …, T. P. Knowles. 2016. Microfluidic diffusion viscometer for rapid analysis of complex solutions. *Anal. Chem.* 88:3488–3493.

24. van Leeuwen, M., X. Li, …, W. M. van Gulik. 2009. Quantitative determination of glucose transfer between concurrent laminar water streams in a H-shaped microchannel. *Biotechnol. Prog.* 25:1826–1832.

25. Hatch, A., E. Garcia, and P. Yager. 2004. Diffusion-based analysis of molecular interactions in microfluidic devices. *Proc. IEEE.* 92:126–139.

26. Kamholz, A. E., and P. Yager. 2001. Theoretical analysis of molecular diffusion in pressure-driven laminar flow in microfluidic channels. *Biophys. J.* 80:155–160.

27. Kamholz, A. E., B. H. Weigl, …, P. Yager. 1999. Quantitative analysis of molecular interaction in a microfluidic channel: the T-sensor. *Anal. Chem.* 71:5340–5347.

28. Yates, E. V., T. Müller, …, T. P. Knowles. 2015. Latent analysis of unmodified biomolecules and their complexes in solution with attomole detection sensitivity. *Nat. Chem.* 7:802–809.

29. Häusler, E., P. Domagalski, …, A. Bardow. 2012. Microfluidic diffusion measurements: the optimal H-cell. *Chem. Eng. Sci.* 72:45–50.

30. Berends, C. 2015. Determination of the diffusion coefficient of phenolic compounds using microfluidics. *In* Department of Biotechnology. Delft University of Technology.

31. Rohsenow, W. M., J. P. Hartnett, and Y. I. Cho. 1998. Handbook of Heat Transfer. McGraw-Hill, New York.

32. Walter, É., and L. Pronzato. 1990. Qualitative and quantitative experiment design for phenomenological models—a survey. *Automatica.* 26:195–213.

33. Kuehner, D. E., C. Heyer, …, J. M. Prausnitz. 1997. Interactions of lysozyme in concentrated electrolyte solutions from dynamic light-scattering measurements. *Biophys. J.* 73:3211–3224.

34. Lehermayr, C., H. C. Mahler, …, S. Fischer. 2011. Assessment of net charge and protein-protein interactions of different monoclonal antibodies. *J. Pharm. Sci.* 100:2551–2562.

35. Kim, M. M., and A. L. Zydney. 2004. Effect of electrostatic, hydrodynamic, and Brownian forces on particle trajectories and sieving in normal flow filtration. *J. Colloid Interface Sci.* 269:425–431.

36. Li, A., and G. Ahmadi. 1992. Dispersion and deposition of spherical particles from point sources in a turbulent channel flow. *Aerosol Sci. Technol.* 16:209–226.

37. Cadman, A. D., R. Fleming, and R. H. Guy. 1982. Diffusion of lysozyme chloride in water and aqueous potassium chloride solutions. *Biophys. J.* 37:569–574.

38. Albright, J. G., O. Annunziata, …, A. J. Pearlstein. 1999. Precision measurements of binary and multicomponent diffusion coefficients in protein solutions relevant to crystal growth: lysozyme chloride in water and aqueous NaCl at pH 4.5 and 25 C⊥. *J. Am. Chem. Soc.* 121:3256–3266.

39. Bauer, K. C., M. Göbel, …, J. Hubbuch. 2016. Concentration-dependent changes in apparent diffusion coefficients as indicator for colloidal stability of protein solutions. *Int. J. Pharm.* 511:276–287.

40. Svanidze, A. V., I. P. Koludarov, …, L.-s. Kan. 2012. Specific features of the temperature behavior of lysozyme diffusivity in solutions with different protein concentrations. *J. Mol. Liq.* 168:7–11.

41. Sorret, L. L., M. A. DeWinter, …, T. W. Randolph. 2016. Challenges in predicting protein-protein interactions from measurements of molecular diffusivity. *Biophys. J.* 111:1831–1842.

42. Grigsby, J., H. Blanch, and J. Prausnitz. 2000. Diffusivities of lysozyme in aqueous MgCl2 solutions from dynamic light-scattering data: effect of protein and salt concentrations. *J. Phys. Chem. B.* 104:3645–3650.

43. Parmar, A. S., and M. Muschol. 2009. Hydration and hydrodynamic interactions of lysozyme: effects of chaotropic versus kosmotropic ions. *Biophys. J.* 97:590–598.

44. Prinsen, P., and T. Odijk. 2006. Fluid-crystal coexistence for proteins and inorganic nanocolloids: dependence on ionic strength. *J. Chem. Phys.* 125:074903.

45. Saluja, A., R. M. Fesinmeyer, …, Y. R. Gokarn. 2010. Diffusion and sedimentation interaction parameters for measuring the second virial coefficient and their utility as predictors of protein aggregation. *Biophys. J.* 99:2657–2665.

46. Hulse, W. L. and R. T.Forbes. Taylor dispersion analysis to gain an insight into formulation buffer salts on the stability and aggregation behaviour of proteins. https://slideplayer.com/slide/5003746/.

47. Tanaka, H., S. Takahashi, …, S. Fukuyama. 2006. Diffusion coefficient of the protein in various crystallization solutions: the key to growing high-quality crystals in space. *Microgravity Sci. Technol.* 18:91–94.

48. Marlowe, R. L. 1983. A study of the concentration dependence of macromolecular diffusion using photon correlation spectroscopy. PhD thesis. University of Cincinnati.

49. Papadopoulos, K. N. 2008. Food Chemistry Research Developments. Nova Science Publishers, New York.

50. Amrhein, S., K. C. Bauer, …, J. Hubbuch. 2015. Non-invasive high throughput approach for protein hydrophobicity determination based on surface tension. *Biotechnol. Bioeng.* 112:2485–2494.

51. Bigelow, C. C. 1967. On the average hydrophobicity of proteins and the relation between it and protein structure. *J. Theor. Biol.* 16:187–211.

52. Curtis, R. A., J. Ulrich, …, H. W. Blanch. 2002. Protein-protein interactions in concentrated electrolyte solutions. *Biotechnol. Bioeng.* 79:367–380.

53. Fair, B., D. Chao, and A. Jamieson. 1978. Mutual translational diffusion coefficients in bovine serum albumen solutions measured by quasielastic laser light scattering. *J. Colloid Interface Sci.* 66:323–330.

54. Hofmeister, F. 1888. About the science of the effects of salts: about the water withdrawing effect of the salts. *Arch. Exp. Pathol. Pharmacol.* 24:247–260.

55. Zhang, Y., and P. S. Cremer. 2006. Interactions between macromolecules and ions: the Hofmeister series. *Curr. Opin. Chem. Biol.* 10:658–663.

56. Tietze, A. A., F. Bordusa, …, A. Stark. 2013. On the nature of interactions between ionic liquids and small amino-acid-based biomolecules. *Chemphyschem.* 14:4044–4064.

57. Salis, A., and B. W. Ninham. 2014. Models and mechanisms of Hofmeister effects in electrolyte solutions, and colloid and protein systems revisited. *Chem. Soc. Rev.* 43:7358–7377.

58. Muschol, M., and F. Rosenberger. 1995. Interactions in undersaturated and supersaturated lysozyme solutions: static and dynamic light scattering results. *J. Chem. Phys.* 103:10424–10432.

59. Minton, A. P. 1997. Influence of excluded volume upon macromolecular structure and associations in 'crowded' media. *Curr. Opin. Biotechnol.* 8:65–69.

60. Saluja, A., and D. S. Kalonia. 2008. Nature and consequences of protein-protein interactions in high protein concentration solutions. *Int. J. Pharm.* 358:1–15.

61. Han, J., and J. Herzfeld. 1993. Macromolecular diffusion in crowded solutions. *Biophys. J.* 65:1155–1161.

62. Dwyer, J. D., and V. A. Bloomfield. 1993. Brownian dynamics simulations of probe and self-diffusion in concentrated protein and DNA solutions. *Biophys. J.* 65:1810–1816.

63. Leaist, D. G. 1987. Counterion-accelerated diffusion of aqueous serum albumin. *J. Solution Chem.* 16:805–812.

64. Gosting, L. J. 1956. Measurement and interpretation of diffusion coefficients of proteins. *Adv. Prot. Chem.* 11:429–554.

65. den Akker, V., and R. F. Mudde. 2014. Transport Phenomena: The Art of Balancing. Delft Academic Press, Delft, the Netherlands.

66. Liu, X., A. Martín-Calvo, …, T. J. Vlugt. 2012. Fick diffusion coefficients in ternary liquid systems from equilibrium molecular dynamics simulations. *Ind. Eng. Chem. Res.* 51:10247–10258.

67. Fowler, K., P. J. Connolly, …, S. O'Meara. 2018. Maxwell–Stefan diffusion: a framework for predicting condensed phase diffusion and phase separation in atmospheric aerosol. *Atmos. Chem. Phys.* 18:1629–1642.

68. Wills, P. R., L. W. Nichol, and R. J. Siezen. 1980. The indefinite self-association of lysozyme: consideration of composition-dependent activity coefficients. *Biophys. Chem.* 11:71–82.

69. Giordano, R., A. Salleo, …, F. Wanderlingh. 1979. Viscosity and density of lysozyme in water. *Phys. Lett. A.* 70:64–66.

70. Arzenšek, D., R. Podgornik, and D. Kuzman. 2010. Dynamic light scattering and application to proteins in solutions. *In* Seminar, Department of Physics. University of Ljubljana, pp. 1–18.

71. Cussler, E. L. 2013. Multicomponent Diffusion. Elsevier, Amsterdam, the Netherlands.

72. Petrásek, Z., and P. Schwille. 2008. Precise measurement of diffusion coefficients using scanning fluorescence correlation spectroscopy. *Biophys. J.* 94:1437–1448.

73. Tian, Y., M. M. Martinez, and D. Pappas. 2011. Fluorescence correlation spectroscopy: a review of biochemical and microfluidic applications. *Appl. Spectrosc.* 65:115A–124A.

74. Elson, E. L. 2011. Fluorescence correlation spectroscopy: past, present, future. *Biophys. J.* 101:2855–2870.

75. Shahzad, A., M. Knapp, …, G. Köhler. 2011. The use of fluorescence correlation spectroscopy (FCS) as an alternative biomarker detection technique: a preliminary study. *J. Cell. Mol. Med.* 15:2706–2711.

76. Aune, K. C., and C. Tanford. 1969. Thermodynamics of the denaturation of lysozyme by guanidine hydrochloride. II. Dependence on denaturant concentration at 25 degrees. *Biochemistry.* 8:4586–4590.

77. van Gelder, B., and E. C. Slater. 1962. The extinction coefficient of cytochrome c. *Biochim. Biophys. Acta.* 58:593–595.

78. Castro-Forero, A., D. Jiménez, …, M. Torres-Lugo. 2008. Immobilization of myoglobin from horse skeletal muscle in hydrophilic polymer networks. *J. Appl. Polym. Sci. Symp.* 107:881–890.

79. Ross, J. R. 1991. Practical Handbook of Biochemistry and Molecular Biology: Edited by G D Fasman. pp 601. CRC Press, Boca Raton, Florida, USA. 1989. $00 ISBN 0–8493–3705–4. *Biochem. Educ.* 19:95–96.

80. Pace, C. N., F. Vajdos, …, T. Gray. 1995. How to measure and predict the molar absorption coefficient of a protein. *Protein Sci.* 4:2411–2423.

81. Hawe, A., V. Filipe, and W. Jiskoot. 2010. Fluorescent molecular rotors as dyes to characterize polysorbate-containing IgG formulations. *Pharm. Res.* 27:314–326.

82. Haynes, W. M. 2014. CRC Handbook of Chemistry and Physics. CRC press, Boca Raton, FL.

83. Dolinsky, T. J., J. E. Nielsen, …, N. A. Baker. 2004. PDB2PQR: an automated pipeline for the setup of Poisson-Boltzmann electrostatics calculations. *Nucleic Acids Res.* 32:W665–W667.

84. Centre for Proteome Research, Liverpool. Buffer calculator. https://www.liverpool.ac.uk/pfg/Research/Tools/BuffferCalc/Buffer.html.

85. Szymański, J., E. Poboży, …, R. Hołyst. 2007. Net charge and electrophoretic mobility of lysozyme charge ladders in solutions of nonionic surfactant. *J. Phys. Chem. B*. 111:5503–5510.

86. Myerson, A. S. 1996. Diffusivity of protein in aqueous solutions. *Korean J. Chem. Eng.* 13:288–293.

87. Kontturi, A. K., K. Kontturi, …, M. Vuoristo. 1992. The effective charge number and diffusion coefficient of cationic cytochrome c in aqueous solution. *Acta Chem. Scand.* 46:348–353.

88. Nozaki, M. 1960. Studies on cytochrome c: IV. mode of existence of native and modified cytochrome c. *J. Biochem.* 47:592–599.

89. Riveros-Moreno, V., and J. B. Wittenberg. 1972. The self-diffusion coefficients of myoglobin and hemoglobin in concentrated solutions. *J. Biol. Chem.* 247:895–901.

90. Choi, J., and M. Terazima. 2002. Denaturation of a protein monitored by diffusion coefficients: myoglobin. *J. Phys. Chem. B*. 106:6587–6593.

91. Gibbs, S. J., A. S. Chu, …, T. W. Root. 1991. Ovalbumin diffusion at low ionic strength. *J. Phys. Chem.* 95:467–471.

92. Scott, D. J., S. E. Harding, and D. J. Winzor. 2014. Concentration dependence of translational diffusion coefficients for globular proteins. *Analyst (Lond.)*. 139:6242–6248.

93. Medda, L., M. Monduzzi, and A. Salis. 2015. The molecular motion of bovine serum albumin under physiological conditions is ion specific. *Chem. Commun. (Camb.)*. 51:6663–6666.

94. Meechai, N., A. M. Jamieson, and J. Blackwell. 1999. Translational diffusion coefficients of bovine serum albumin in aqueous solution at high ionic strength. *J. Colloid Interface Sci.* 218:167–175.

95. Jøssang, T., J. Feder, and E. Rosenqvist. 1988. Photon correlation spectroscopy of human IgG. *J. Protein Chem.* 7:165–171.